

Diffusion model for iontophoresis measured by laser-Doppler perfusion flowmetry, applied to normal and preeclamptic pregnancies

Frits F. M. de Mul

University of Groningen
University Medical Center Groningen
Faculty of Medicine
Department of Biomedical Engineering
Anthonius Deusinglaan 1
9713 AV Groningen
The Netherlands
E-mail: f.f.m.de.mul@med.umcg.nl

Judith Blaauw

Jan G. Aarnoudse

University of Groningen
University Medical Center Groningen
Faculty of Medicine
Department of Obstetrics and Gynecology
Anthonius Deusinglaan 1
9713 AV Groningen
The Netherlands

Andries J. Smit

University of Groningen
University Medical Center Groningen
Faculty of Medicine
Department of Internal Medicine
Anthonius Deusinglaan 1
9713 AV Groningen
The Netherlands

Gerhard Rakhorst

University of Groningen
University of Medical Center Groningen
Faculty of Medicine
Department of Biomedical Engineering
Anthonius Deusinglaan 1
9713 AV Groningen
The Netherlands

1 Introduction

Iontophoresis is the introduction of charged substances into the skin by means of a small electrical current. It is based on the principle that a charged molecule migrates under the influence of an applied electrical field toward electrodes of opposite charge placed on tissue. Normally, one electrode consists of a conductive sponge, containing the material to be introduced. The other electrode is located some distance from the first one. A comprehensive review of the method, together with pharmaceutical, physiological, and experimental details, has been published by Banga.¹

Laser-Doppler perfusion flow monitoring (LDPM) measures the averaged blood flow in small dermis vessels. Coher-

Abstract. We present a physical model to describe iontophoresis time recordings. The model is a combination of monodimensional material diffusion and decay, probably due to transport by blood flow. It has four adjustable parameters, the diffusion coefficient, the decay constant, the height of the response, and the shot saturation constant, a parameter representing the relative importance of subsequent shots (in case of saturation). We test the model with measurements of blood perfusion in the capillary bed of the fingers of women who recently had preeclampsia and in women with a history of normal pregnancy. From the fits to the measurements, we conclude that the model provides a useful physical description of the iontophoresis process. © 2007 Society of Photo-Optical Instrumentation Engineers. [DOI: 10.1117/1.2671053]

Keywords: iontophoresis; flowmetry; pregnancy; laser-Doppler; tissue perfusion; preeclampsia.

Paper 06110R received Apr. 26, 2006; revised manuscript received Sep. 12, 2006; accepted for publication Sep. 13, 2006; published online Mar. 1, 2007.

ent light from a laser partly scatters in moving red blood cells before emerging at the tissue surface. Due to the Doppler effect, the frequency of the light will slightly change according to the velocity of the cells. A photodiode, measuring both the original laser light and the Doppler-shifted emerged light, will produce a Doppler frequency signal. The strength of this signal depends on the moving blood cell flow.

The combination of LDPM and iontophoresis offers an opportunity to assess changes in the cutaneous microcirculation after administration of vaso-active drugs without systemic effects. Iontophoresis of sodium nitroprusside (SNP), donating directly nitric oxide, is commonly accepted to provoke endothelium-independent vasodilatation, whereas iontophoresis of acetylcholine chloride (ACh) is commonly used to test endothelium-dependent vasodilatation. The methodology us-

Address all correspondence to Frits de Mul, University of Groningen, Faculty of Medicine, Department of Biomedical Engineering, Anthonius Deusinglaan 1, 9713 AV Groningen, The Netherlands; E-mail: f.f.m.de.mul@med.umcg.nl

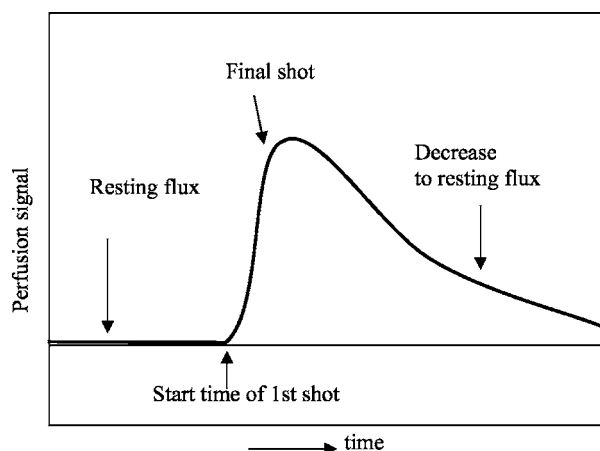


Fig. 1 Typical time recording of an iontophoresis provocation, as measured with laser-Doppler perfusion flowmetry.

ing iontophoresis and laser-Doppler flowmetry has been widely used to investigate microvascular function in various vascular disease states, most commonly in diabetes mellitus.^{2,3}

Endothelium activation or dysfunction plays an important role in the clinical manifestations and pathophysiology of preeclampsia, a serious pregnancy complication characterized by hypertension, proteinuria, increased peripheral resistance, and reduced organ perfusion. By using iontophoresis and laser-Doppler flowmetry, increased responses of acetylcholine were found in preeclampsia compared to normotensive women.⁴ We previously showed that even 6 to 7 months after delivery, ACh-mediated reactivity was observed to be increased in women with a history of early-onset preeclampsia.⁵

Until now, clinical iontophoresis research has exclusively concentrated on the relative height of the excess perfusion signal, compared with that of the flux in resting conditions (the “resting flux”). However, when comparing time recordings of various groups of patients and healthy (control) persons, we observed differences in the shape of the time recordings, in particular in the characteristic times of the onset of the excess perfusion and of the return to resting flux conditions. Therefore, we decided that it was worthwhile to investigate these differences more thoroughly, and for that purpose, we need means to quantify characteristics based on a physically sound model.

A typical time recording of a laser-Doppler perfusion measurement during the iontophoresis process is shown in Fig. 1. The measurement starts with a recording of the resting flux. This is followed by a series of shots, in which the electrical current is applied. The result is an enhanced perfusion signal climbing to a maximum value. After the shots, the perfusion signal returns to the resting flux value.

The model should be able to describe the diffusion process of the drug material into tissue. This process is governed by the diffusion coefficient (expressed in m^2/s). In the case of laser-Doppler iontophoresis measurements, the dimensions of the optical probe are very small compared to those of the exchange area, and thus we can describe the diffusion process into tissue, as far as can be seen by the laser probe, as a monodimensional process.

The model should also admit leakage of drug material due to transport by blood flow out of the tissue under the iontoprobe. However, this diffusion model does not include leakage of material other than toward infinite depth, and thus we have to include an extra term for that purpose. Therefore, we insert a decay function analogously to radioactive decay. Further, since iontophoresis protocols frequently consist of several subsequent shots, the model should take care of this. Finally, the model should be maximum protocol independent.

In the literature, some modeling of normal (not electrically sustained) diffusion of molecules through membranes into tissue has been published.¹ Most models rely on Fick’s law⁶ of material diffusion in one dimension. Flynn⁷ gives an overview of several of these models, together with experimental data of the permeability coefficients P (in cm/h) and the partition coefficients K (dimensionless) for the material transfer at the octanol/water partition, which is supposed to resemble the stratum-corneum/water partition. He also indicates the relation with the diffusion coefficient D (in cm^2/s):

$$P = KD/h, \quad (1)$$

where h is the thickness of the membrane. This thickness is normally taken as about 0.5 mm for tissue epidermis,⁸ and 500 nm for lipid layers.⁹ The latter authors also investigated the permeability results of Flynn and others in extensive detail.

A purely phenomenological model for iontophoresis diffusion was presented by Özbek et al.⁹ It consisted of one or two hyperbolic time functions, but without underlying physical argumentation. This model only tries to describe the onset of excess flow after the start of administering the material, but not the whole time recording.

The study was a part of a broader investigation of pregnant and nonpregnant women, with or without hypertension, during or after pregnancy.⁵ Since our present objective is to present the model, we only present data for patients and control persons postpartum. Other measurements will be published elsewhere.

2 Model

Perfusion changes after iontophoresis were measured with laser-Doppler perfusion flowmetry. Upon administering drugs like ACh or SNP, a change in the blood perfusion is measured. We assume that microvascular capillaries react by vasodilatation, thus enlarging the blood perfusion either by an increase in the number of moving red blood cells or by an increase in their velocities. In both ways the transport of the administered drug out of the region under examination will be favored.

The iontophoresis process is determined by the geometry of the iontophoresis/laser-Doppler probe and the tissue region that is measured. Normally, the probe will contain two (or more) glass fibers for transport of the laser light, one for light supply and one (or more) for the reflected light (see Fig. 2). At the tissue surface, these fibers are positioned at standardized separation distances (here 250 μm). The diameter of the fibers is typically 100 to 200 μm . The fibers are placed in the center of a larger container, with typical diameters of 10 to 20 mm and height of 10 mm. The container is filled with sponge-like material, fit to store the drug to be administered, and in electrical contact with the tissue. An electrode is con-

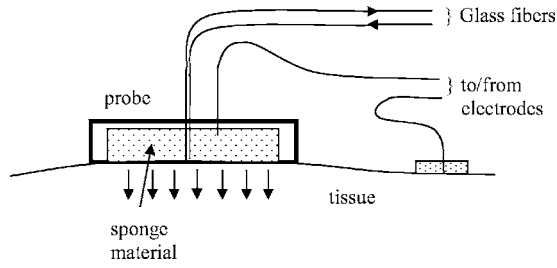


Fig. 2 Schematic view of an iontophoresis laser-Doppler perfusion flow probe. Typical dimensions are: probe, diam 10 to 20 mm and height 5 to 10 mm; fiber separation, 250 μm . The diffusion can be considered as monodimensional.

nected to the sponge material, with another electrode to be connected to the patient at a different place. The drug itself must be electrically conductive. Upon applying a voltage difference over the two electrodes, the drug will be part of the electrical circuit, and ionized molecules of the drug may diffuse into the tissue. The number of molecules that actually have diffused into the tissue can be estimated by registration of the electric current strength and its time duration.

For the transport of drug molecules, we assume that two mechanisms are present. The first is the diffusion of the administered molecules from the probe into the tissue. Since the separation between the two (sets of) glass fibers is small compared with the dimensions of the sponge material in the probe, we may consider the diffusion process as effectively 1-D, with the depth z ($z > 0$) into tissue as the coordinate variable. In such cases the well-known diffusion equation⁶ reads

$$\frac{\partial c}{\partial t} = D \frac{\partial^2 c}{\partial z^2}, \quad (2)$$

with t as the time, $c(z, t)$ as the concentration (kg/m^3), and D as the diffusion coefficient (m^2/s).

This differential equation can be solved by introducing the boundary conditions:

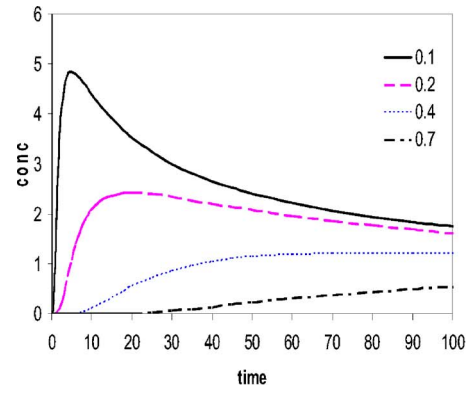
$$\begin{aligned} \text{for times } t < 0: & \quad c(z, t) = 0, \text{ and} \\ \text{at zero time} & \quad c(z, 0) = c_0 \cdot \delta(0, 0), \end{aligned}$$

$$\text{with } \int_0^\infty c(z, t) \cdot dz = Q \text{ for all } t, \text{ including } t = 0. \quad (3)$$

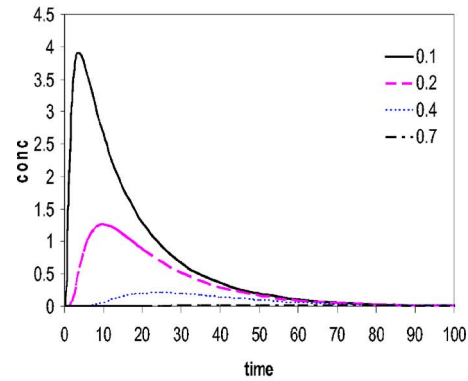
Q stands for the total mass of material that is injected per m^2 tissue surface area under the probe. Equation (3) means that at $t=0$, a single shot is delivered at the boundary of the tissue, with a very short duration (a delta pulse). Then the solution of Eq. (2) is

$$c(z, t) = \frac{Q}{\sqrt{\pi Dt}} \exp\left\{-\frac{z^2}{4Dt}\right\}. \quad (4)$$

In iontophoresis protocols, frequently a number of shots is administered. We deal with that shortly. In Fig. 3(a), this diffusion function is sketched for inspection. It is seen that for chosen values of z , the function first will increase and finally decrease to zero.



(a)



(b)

Fig. 3 The diffusion function, Eq. (4), plotted as a function of time for several values of the depth as the parameter. $Q=1$ and $D=0.001$, (a) without decay factor and (b) with decay constant $\lambda=0.05$. All variables and parameters are dimensionless here.

The time functions decrease toward zero slowly, which is due to the absence of leakage of material, other than toward $z \rightarrow \infty$. In reality we have leakage of molecules out of the measured volume (in pharmacokinetics “distribution”), due to transport by blood perfusion (“elimination”). More generally, the effect of the molecules on the perfusion may decrease in time, either due to removal or to saturation effects or reduction in efficiency (“tolerance”). This presents an extra term in the differential equation, analogous to the term representing decay, as with radioactive decay, or with a decrease of gas concentrations using ventilation. With this extra term, the equation reads:

$$\frac{\partial c}{\partial t} = D \frac{\partial^2 c}{\partial z^2} - \lambda c, \quad (5)$$

with λ as the decay constant ($\lambda > 0$), related to the “half-value time” $T_{1/2}$ by $T_{1/2} = \ln 2 / \lambda$. The solution of the decay part of Eq. (5) (with $D=0$) is

$$c(t) = c(0) \exp(-\lambda t), \quad (6)$$

the well-known exponential decay function. The final solution of Eq. (5) is

$$c(z,t) = \frac{Q}{\sqrt{\pi Dt}} \exp\left\{-\frac{z^2}{4Dt} - \lambda t\right\}. \quad (7)$$

This expression can be derived analytically using Laplace-transformation techniques. The validity can be verified by the insertion of Eq. (7) into Eq. (5). Figure 3(b) presents a sketch of this solution for a nonzero value of the decay constant λ .

A comparison of these two figures shows a faster decrease from maximum toward zero when we include the decay function into the expression.

The maximum of the function of Eq. (7) is found at

$$t_{\max} = \frac{1}{4\lambda} \left[-1 + \sqrt{1 + \frac{2z^2\lambda}{D}} \right], \quad (8)$$

which reduces to $z^2/(4D)$ when λ is very small (i.e., slow washout). The actual amplitude of the maximum can be found by insertion of t_{\max} in Eq. (7).

The next step assumes that the flow, as measured using laser-Doppler perfusion flowmetry, is proportional to the concentration of administered drug molecules. This technique measures the average blood flow F , which can be considered as the (averaged) product of the concentration of moving red blood cells and their velocities (see Sec. 3 for experimental details). According to our remarks in Sec. 1, we assume that the excess blood flow ΔF upon drug injection, i.e., the increase of the flow above its level in resting conditions, is proportional to the actual concentration of drug molecules. With this assumption we arrive at the expression

$$\Delta F(t) = \frac{Q_0}{\sqrt{\pi Dt}} \exp\left(-\frac{z^2}{4Dt} - \lambda t\right), \quad (9)$$

with Q_0 as a constant related to the maximum value. We adopted this expression for comparison with our experimental data. In this way, the variable z represents an average depth for the diffusion and decay process to take place.

Normally in iontophoresis, a series of shots is delivered instead of a single shot. For repeated shots, the start condition of zero concentration at all depths is not valid any more. This may lead to a process of saturation, since the concentration at low depths will increase with time, which eventually (at high concentrations) might hamper new molecules to diffuse inward. Another cause for saturation might be the limited capacity of the vessel wall to incorporate iontophoresis molecules, which might reduce the flow. As a first approximation, we take that into account using

$$\Delta F(t) = \sum_{n=1}^N \exp[-(n-1)s] \frac{Q_0}{\sqrt{\pi Dt_n}} \exp\left(-\frac{z^2}{4Dt_n} - \lambda t_n\right); \quad (10)$$

$$t_n = t - (n-1)\Delta t,$$

where n stands for the shot number ($n=1 \dots N$), s is a constant accounting for the saturation effect, t_n is the time of the n th shot, and Δt is the time interval between the shots. The summation is taken for positive t_n values only. When s is zero, all shots contribute equally, albeit time-shifted (and the time record will start smoothly). When s is much larger than unity, only the first shot contributes (and the time record starts more abruptly).

For the fitting process we used the function:

$$\Delta F = \sum_{n=1}^N \exp[-(n-1)s] \frac{C}{\sqrt{t_n/t_h}} \exp\left[-\frac{\tau_1}{t_n} - \frac{t_n}{\tau_2}\right];$$

$$C = \frac{Q_0}{\sqrt{\pi D}}; \quad \tau_1 = \frac{z^2}{4D}; \quad \tau_2 = \frac{1}{\lambda}, \quad (11)$$

with s , C , τ_1 , and τ_2 as the parameters to be fitted. The parameter τ_1 combines the model parameters z , which here has a role of an “effective perfusion depth,” and D , the “apparent diffusion constant.” Larger τ_1 and τ_2 values indicate slower diffusion and slower decay (or washout), respectively. The constant t_h is included for dimensional purposes. It is taken as half of the period, over which we perform the fitting process. All times are measured from the start of the first shot t_{begin} .

Since in the protocols the duration of each shot is finite (no delta-like pulses), we took that into account by dividing each shot into short subsequent subshots, calculating the contribution of each subshot using time shifting, and summing up all those partial contributions.

We applied as the fitting scheme: minimization of the standard χ^2 value, calculated from the squared differences between the measured values and the corresponding function values, each divided by the squared standard deviation σ at that measured value, and summed over all measured points. The summation extends over the time region between the starting point t_{begin} of the iontophoresis and a chosen time point when the measured values have returned to the level of the resting flux values or when the occlusion starts. We calculated the standard deviations in each measuring point from the deviations of the measured values and calculated values using a cubic polynomial approximation, averaged over a relatively large number (about -60 to $+60$) of surrounding measuring points. The χ^2 fit was performed by repeated subsequent stepwise variation of each parameter around its actual value, i.e., at that value, and at the value plus or minus the step size, respectively. When in that process the smallest χ^2 value appeared at one of these three parameter values, we adopted that value as the new “actual value” and multiplied the parameter step size with a factor $1/\sqrt{2}$, $\sqrt{2}$, or again $\sqrt{2}$, respectively. To avoid being trapped in local minima during the fitting process, we frequently multiplied the step sizes by a factor of 10 or 100. The fit was continued until eventually no relative change larger than 10^{-6} in χ^2 was observed. To start the fitting process, we inserted initial parameter values manually or by using a coarse first estimation (e.g., $s=0.5$, and τ_1 and τ_2 equal to the apparent rise time or decay time of the response signal). Since for the model the maximum value cannot be calculated analytically, one might take the apparent maximum of the response curve as the default starting value.

For an ideal fit, the reduced χ^2 , calculated from that standard χ^2 by division by the difference of the number of measured points and the degrees of freedom (the number of model variables, actually 4), should approach unity as its minimum value. When one of the parameters is varied until the reduced χ^2 equals the minimum value $+1$, that variation indicates the standard deviation σ in that parameter value. This σ was calculated afterward for all parameters, for each individual re-

cording. For each group of subjects, the standard deviation was calculated afterward by standard methods.

We included an option for a Gaussian weighting filter $f_{\text{corr}}(t)$ for the points:

$$f_{\text{corr}}(t) = \exp[-(t/t_h)^2]; \quad t_h = (t_{\text{end}} - t_{\text{begin}})/2, \quad (12)$$

with t_{begin} and t_{end} as the starting and end time points of the fit, respectively (all times are measured from the starting point). However, it turns out that applying this filter has only a slight effect on the resulting parameter values. This can be understood by realizing that most significant contributions to χ^2 appear for small times t .

3 Measurements

Skin perfusion was measured by a Periflux 4000 laser-Doppler system in combination with a Periflux tissue heater set to 31°C (PF4005, Peritemp), with all equipment from Perimed, Sweden. A laser beam (wavelength of 780 nm) is conducted through optical fibers to illuminate the skin. As the precise investigated volume is unknown, the signal collected by the returning fiber is expressed in arbitrary units and referred to as flux (PU). The vascular measurements were performed with the subjects in a sitting position, their forearms on a soft pillow at heart level, in a temperature-controlled room ($T=23.4\pm 0.5^\circ\text{C}$). Tissue temperature was recorded during the measurements. Caffeine-containing drinks and smoking were not allowed 2 h prior to the test.

A special iontophoresis probe (PF481-2, Perimed, Sweden) containing a thermostatic probe holder was placed on the dorsal side of the middle phalanx of the third finger. A second probe was placed at the first phalanx of the same finger and measured the blood perfusion without being influenced by the administration of the drugs.

A battery-powered iontophoresis controller (PeriIont 382, Perimed, Sweden) was used to provide a direct current for drug iontophoresis. The monitor's signal processing electronics calculates the zero and first moments, M_0 and M_1 , of the frequency power spectrum $S(\omega)$ of the measured ac-signal $f(t)$:

$$M_n = \int_{\omega_1}^{\omega_2} \omega^n S(\omega) d\omega; \quad n=0,1, \quad (13)$$

with ω_1 and ω_2 as the bandwidth limits (set at 20 Hz to 12 kHz). This calculation is done in the time domain, and corresponds to the zero-time autocorrelation values of the signal and its derivative, respectively. From $M_1(t)$ the perfusion flow is obtained after division (normalization) with the square of the total reflection from the sample. $M_0(t)$ can be considered as a measure for the concentration of moving scattering particles (red blood cells). In this study, we did not use this function. A PC equipped with a data-acquisition subsystem recorded the analog outputs of the monitor at a rate of 40 measurements per second. The data files were processed for conversion from mV to perfusion units (PU) by division with the gain factor of the instrument (10 mV/PU). Afterward, the data were averaged per 40 samples to remove heart beat fluctuations. This resulted in data at 1-s intervals.

Table 1 Experimental settings. ACh=acetyl choline chloride, $(\text{CH}_3)_3\text{N}(\text{Cl})\text{CH}_2\text{CH}_2\text{OCOCH}_3$, $M=182$, in Miochol. SNP=sodium nitroferricyanide(III), $\text{Na}_2(\text{Fe}(\text{CN})_5\text{NO})\cdot 2\text{H}_2\text{O}$, $M=298$. ⁽¹⁾ 100 or 200 s in later measurements; ⁽⁰⁾ between begin times of shots.

	Code	ACh	SNP
Subjects		Number	Number
Preeclampsia patients (postpartum)	PPP	22	20
Controls (healthy) (postpartum)	PPC	18	21
Resting flow measurement, duration (s)		600 ⁽¹⁾	600 ⁽¹⁾
Shot duration (s)		20	20
Current (mA), anodal (A), or cathodal (C)		0.1 A	0.2 C
Number of shots		7	9
Shot interval (s) ⁽⁰⁾		60	90
Duration of occlusion (s)		180	180

The laser-Doppler perfusion measurements were performed using a standardized protocol,^{2,3,10} including:

- resting flow, for a duration Δt_r ,
- N shots, with current I , each with a duration of Δt_s and with time intervals of Δt_i (measured between the respective start times of the shots)
- at about 5 to 10 min after the end of the last shot, start of an arterial occlusion for 3 min
- release of the occlusion, followed by a measurement of the return to resting flow condition.

The occlusion period provided the biological zero signal level. This level was subtracted from the perfusion signal before all further calculations.

Women with Caucasian skin type participated in this study: 25 women with a history of early onset preeclampsia and 23 healthy women with uncomplicated pregnancies. Not all recordings appeared useful; a few recordings from both groups had to be discarded due to disturbing signal artifacts. Preeclampsia was defined according to the criteria of the International Society for the Study of Hypertension in Pregnancy: the appearance of a diastolic blood pressure (DBP) ≥ 90 mmHg measured at two occasions at least 4 h apart in combination with proteinuria (≥ 300 mg/24 h or 2+ dipstick) developing after a gestational age of 20 weeks in a previously normotensive woman. All women had singleton pregnancies and were tested between 3 and 11 months postpartum. None of the participants used any medication during the studies. Women with pre-existing hypertension (blood pressure before 20 weeks of gestation $\geq 140/90$ mmHg or using antihypertensive medication), diabetes mellitus, renal disease, preeclampsia in a previous pregnancy, or who were using vasoactive drugs were excluded. The experimental procedure and the population of subjects were previously described in detail by Blaauw et al.⁵ In Table 1 we summarized the experimental settings.

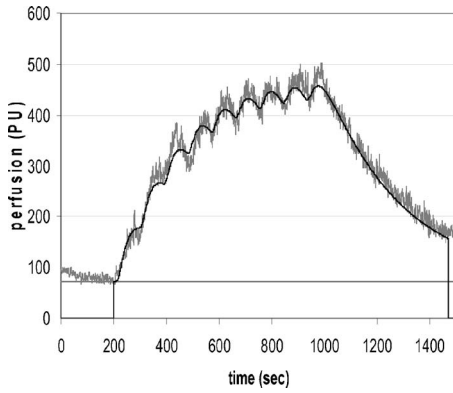


Fig. 4 Typical fit of a laser-Doppler iontophoresis recording of SNP administration, together with the resting flux line (extrapolated from $t < 200$ s) and the fitted line. Parameters: $\chi_{\text{red}}^2 = 1.15$; $\tau_1 = 76 \pm 10$ s; $\tau_2 = 408 \pm 30$ s; and $s = 0.029 \pm 0.014$.

4 Results and Discussion

In Fig. 4 we present a typical example of a time recording of one of the patients. It is seen that upon drug administration, the flux increases sharply from the resting flow level, followed by a much slower decrease toward the resting flow level. The effect of the multiple shots is clearly seen.

We discuss the results in two ways. First, in physical terms, which comprises the validation of the fitting procedure, together with an evaluation of the reduced χ^2 values. Second, we briefly discuss the clinical relevance.

4.1 Physical Analysis

The model was fitted to all recordings of the two groups. For these measurements, we did not use the Gaussian fitting filter, given in Eq. (12). In Fig. 4 the fitted model is shown, together with the measured data and the resting flux line. The fitting program offers the option to include the starting time point as an extra parameter, but with these measurements we fixed the starting time to the values given in Table 1.

After fitting the model to the individual recordings, averaged values were calculated, in which the reduced χ^2 values might be used as weighting factors, according to:

$$\langle P \rangle = \frac{\sum_{i=1}^N \frac{P_i}{\chi_i^2}}{\sum_{i=1}^N \frac{1}{\chi_i^2}}, \quad (14)$$

where P stands for each of the parameters or results of the fit, and i counts for the subjects in the groups ($i = 1 \dots N$). The approximated standard deviation in $\langle P \rangle$ was calculated using the standard formula.

In Fig. 5 we show an overview of the fitted parameters for one of the groups. From that figure it is seen that all χ_{red}^2 values are close to the ideal value of 1. All parameter values show a consistent behavior, apart from:

- the function value C (which is distinct from the apparent curve maximum M), which varies significantly
- the shot saturation constant, which is larger than 10^6 (the artificially set maximum for the parameter values during the fitting process) for subject 9. This subject was excluded from the calculation of the average of that parameter over the group.

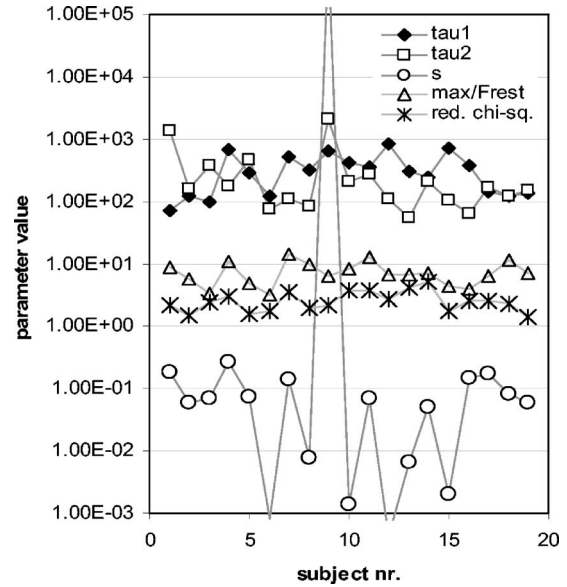


Fig. 5 Overview of results for the fitted parameters for one of the four groups of subjects: the patients with SNP as the administered drug (PPP-SNP). Points: $\blacklozenge = \tau_1$; $\square = \tau_2$; $\circ = s$; $\triangle = \text{max}/F_{\text{rest}}$; $\times = \chi_{\text{red}}^2$. max = maximum value of the fitted curve; F_{rest} = resting flux value. Lines drawn to guide the eye. Subject 9 has an s -value $> 10^6$ (i.e., first shot contributes only).

Additionally, with some subjects (in other groups), the decay parameter τ_2 may rise above that maximum value during the fit. Those subjects were also excluded in the calculation of the averaged τ_2 value of that group. Table 2 shows an overview of the number of excluded subjects per group. It is remarkable, however, that while one of the parameters grows to a large value, the other parameters remain within limits, comparable to the values obtained with other subjects. We have to investigate that point more closely.

In Fig. 6 the averaged values of the fit parameters are shown. The error bars indicate the standard deviations in these averages (or standard errors in the means). Recalculation of the averages, without applying the χ^2 weighting, resulted for all variables and all groups in shifts $< 5\%$, thus within the standard deviation range. The averaged χ^2 values over the four groups are between 1 and 2.5, indicating fits with deviations from the measured data, ranging from equal to about twice the standard deviation in those measured data. We conclude that the fitting procedure worked satisfactorily.

From Fig. 6 it is seen that the groups of patients show larger values for the diffusion time constant τ_1 than the corresponding control groups, meaning that the diffusion will take place over a longer time scale. The values for τ_2 show a pattern that indicates that with ACh the removal (or decay)

Table 2 Excluded subjects in the groups for the calculation of the group average of the parameters s and τ_2 , respectively.

	PPP-ACh	PPC-ACh	PPP-SNP	PPC-SNP
$s \geq 10^5$	3 of 21	1 of 18	1 of 19	2 of 20
$\tau_2 \geq 10^5$ s	1 of 21	1 of 18	0 of 19	2 of 20

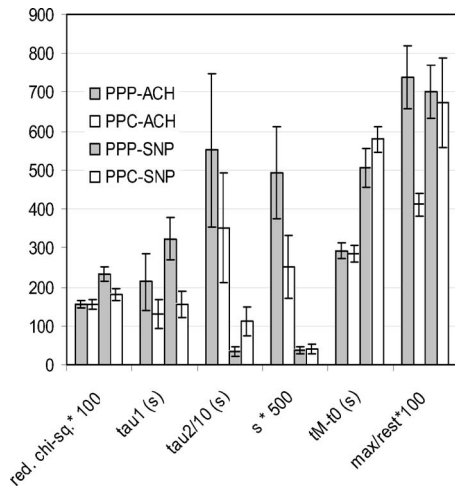


Fig. 6 Averaged parameter values over the four groups of subjects, calculated with χ^2 weighing. max=maximum value of the curve. rest=resting flux. Also included: time t_M from start of iontophoresis to the top of the curve. Error bars indicate standard deviations in the averaged values.

time is longer than with SNP. The shot saturation constant s is large for ACh but small for SNP. This means that with SNP, all shots do contribute, but for with ACh, only the first few shots contribute. The values for t_M also reflect this behavior: with SNP it takes more time to reach the maximum than with ACh. The ratios of the maxima and the resting fluxes appear to show differences for the ACh-administered control group persons, compared with the other groups.

From the time parameter τ_1 we may calculate the apparent diffusion coefficient D , using Eq. (10), provided we insert a proper value for the “effective perfusion depth z .” Assuming $z=1$ mm, we obtain diffusion coefficient values as given in Table 3.

Also in Table 3, half-life decay times $T_{1/2}$, from $T_{1/2} = \ln 2/\lambda = \ln 2\tau_2$, are shown. These times indicate the time needed for removal of half the actual concentration.

We compared the values for the diffusion coefficient with the literature data. From Flynn’s tables⁸ for normal (not electrically sustained) diffusion over membranes, we can estimate permeability constants and from those, using Eq. (1), diffusivities (diffusion constants), which are in the order of 10^{-10} cm²/s. To do this, we calculated the diffusivity D for

Flynn’s whole list of permeability data of about 100 compounds, using Eq. (1) with $h=0.5$ mm,⁹ and interpolated the results at the molecular weight values of ACh and SNP. The logarithmic relation in Eq. (6) of Ref. 9, including the molecular weight, led to similar results.

When we choose $z=1$ mm, the diffusion coefficients for iontophoresis diffusion, which is electrically sustained, are about 4 orders of magnitude larger than the free, nonsustained diffusion coefficient values. This may lead to the establishment of an “iontophoresis diffusion amplification factor,” which could be about 10^4 , using the values indicated earlier.

4.2 Clinical Analysis

A primary analysis of the microvascular measurements, based on manual estimation of the ratio of maximum flux and resting flux, has been presented by Blaauw et al.⁵ Using the model, we are able to add data about the time constants for diffusion and decay, τ_1 and τ_2 , respectively, the saturation constant s , maximum flux, vasodilatation expressed as relative increase in flux from the resting flux obtained by the model (Figs. 7 and 8), and the time interval from start of the iontophoresis and time of reaching maximum flux. Figures 7–9 were obtained without the χ^2 weighing.

We used a Komolgorov-Smirnov test to assess the normality of the data. Since all parameters turned out to be non-normally distributed, the nonparametric Mann-Whitney test was used for testing group differences. To investigate how well the endpoint parameters for the vasodilatation obtained manually and using the model fit agreed, the difference between the two methods was plotted against the average of both methods (Fig. 9). We used the SPSS-software package, version 12.0.1. Significance was accepted at $p < 0.05$.

Microvascular reactivity was tested in 25 recently pre-eclamptic women and 23 controls. Of these 96 measurements, 18 were discarded, as they did not fit in the model, resulting in a total of 21 measurements in the PPP-ACh group, 19 measurements in the PPP-SNP group, 18 measurements in the PPC-ACh group, and 20 measurements in the PPC-SNP group. In the case of the parameters τ_2 and s , few measurements were discarded, as they fell totally out of range (Table 2).

With respect to iontophoresis of ACh, women with recent preeclampsia showed significantly higher values for vasodilatation (Fig. 8), as we presented and discussed before. No sig-

Table 3 Apparent diffusion coefficients for effective perfusion depths of 1 mm, and half life times for decay or removal (with standard deviations of the average; values calculated with χ^2 weighing).

	PPP-ACh		PPC-ACh		PPP-SNP		PPC-SNP	
	Value	SD	Value	SD	Value	SD	Value	SD
τ_1 (s)	214	73	130	38	324	55	156	34
D (10^{-6} cm ² /s)	11.7	4.0	19.2	5.6	7.7	1.3	16.0	3.5
τ_2 (s)	5511	1970	3515	1415	348	118	1121	369
$T_{1/2}$ (s)	3820	1366	2436	981	241	82	777	256

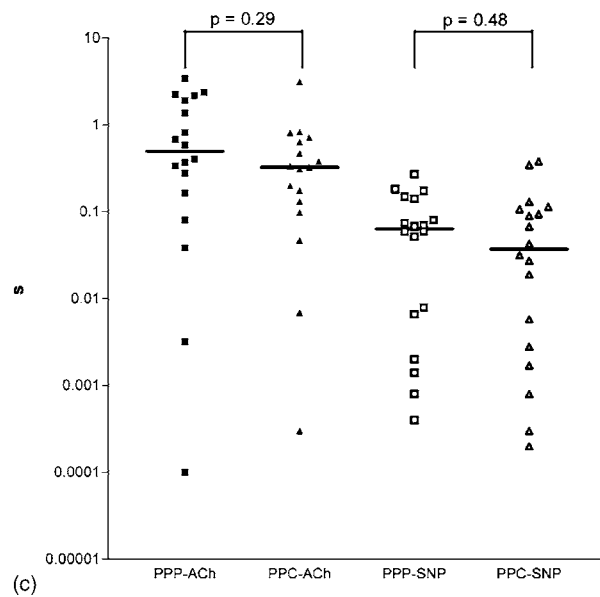
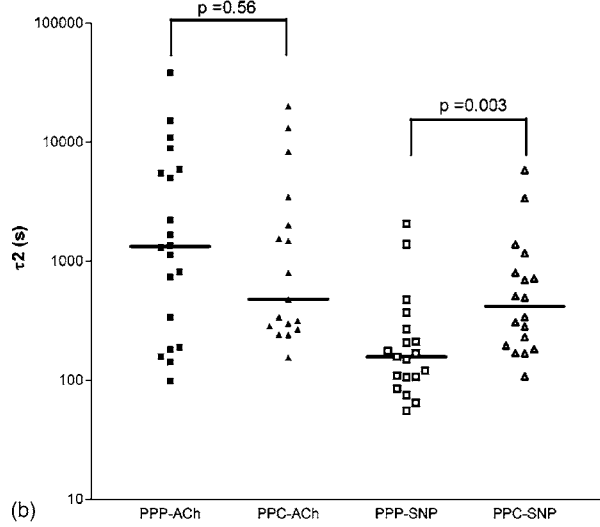
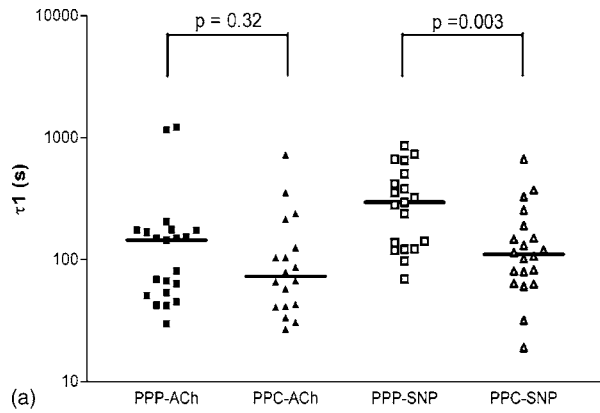


Fig. 7 Measured data for the diffusion time constant τ_1 , the decay time constant τ_2 , and the saturation constant s , with probability values p .

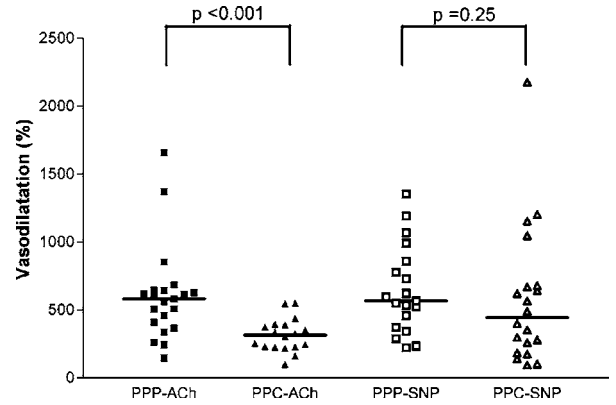


Fig. 8 Vasodilatation (percent), or the maximum excess flux (above the resting flux), relative to that resting flux level.

nificant differences were noticed for the other parameters (Figs. 7–9).

With respect to iontophoresis of SNP, significantly higher values for τ_1 [Fig. 7(a)] were found, whereas lower values for τ_2 [Fig. 7(b)] were noticed for the formerly preeclamptic group compared to the controls. This indicates that diffusion of SNP takes a longer time and the decay or washout of SNP in the formerly preeclamptic group takes shorter times than in the control group.

5 Conclusions

We introduce a physical model to describe the iontophoresis process, as applied to normal and preeclamptic pregnancies. We derive characteristic times for diffusion and for decay (washout and/or saturation). We are able to properly account for the subsequence of iontophoresis shots, used in administering the drugs to the tissue of the subjects.

We see differences in the time recordings of the groups of patients and control persons, and in the type of administered material. These differences are quantified using the variables

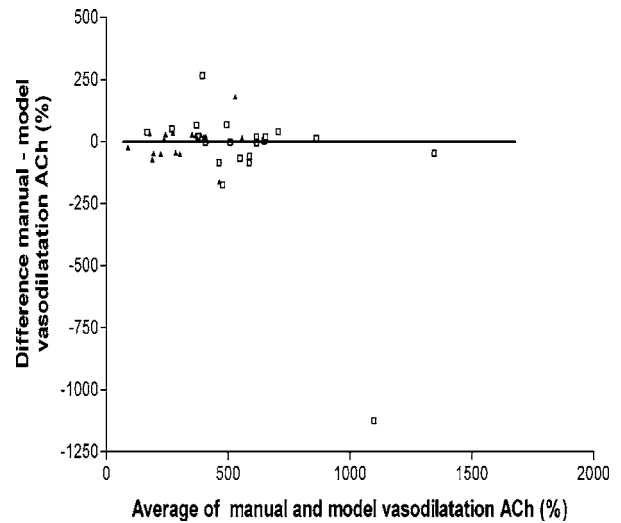


Fig. 9 Difference between vasodilatation (percent) obtained manually and using the model procedure, plotted against the average of the two methods.

of the physical model. Results of further investigations, including other groups of patients, will be published elsewhere.

Frequently, iontophoresis experiments cannot easily be compared due to differences in the clinical protocols adopted by various experimentalists. We hope that this model might help in the future when comparing and interpreting those iontophoresis measurements, and in standardizing protocols for measurements and procedures for analysis of the experimental data.

As a general conclusion, this modeling of the iontophoretic diffusion might offer the opportunity to derive diffusion coefficients and time constants, which may provide a better insight into iontophoretic processes in tissue.

References

1. A. K. Banga, *Electrically Assisted Transdermal and Topical Drug Delivery*, Taylor and Francis, London (1998).
2. S. J. Morris, A. C. Shore, and J. E. Tooke, "Responses of the skin microcirculation to acetylcholine and sodium nitroprusside in patients with NIDDM," *Diabetologia* **38**, 1337–1344 (1995).
3. E. H. Serne, C. D. Stehouwer, J. C. ter Maaten, P. M. ter Wee, J. A. Rauwerda, and A. J. Donker, "Microvascular function relates to insulin sensitivity and blood pressure in normal subjects," *Circulation* **99**, 896–902 (1999).
4. K. R. Davis, J. Ponnampalam, R. Hayman, P. N. Baker, S. Arulkumaran, and R. Donnelly, "Microvascular vasodilator response to acetylcholine is increased in women with preeclampsia," *Br. J. Obstet. Gynaecol.* **108**, 610–614 (2001).
5. J. Blaauw, R. Graaff, M. G. van Pampus, J. J. van Doormaal, A. J. Smit, G. Rakhorst, and J. A. Aarnoudse, "Abnormal endothelium-dependent microvascular reactivity in recently preeclamptic women," *Obstet. Gynecol. (N.Y., NY, U. S.)* **105**(3), 626–632 (2005).
6. A. Fick, "Über Diffusion," *Ann. Phys. Chem.* **94**, 59 (1855).
7. G. L. Flynn, "Physicochemical determination of skin absorption," in *Principles of Route-to-Route Extrapolation for Risk Assessment*, T. R. Gerrity and C. J. Henry, Eds., pp. 93–127, Elsevier, New York (1990).
8. R. O. Potts and R. H. Guy, "Predicting skin permeability," *Pharm. Res.* **9**, 663–669 (1992).
9. F. Y. Özbekit, F. Esen, S. Gülec, and H. Esen, "Evaluation of forearm microvascular blood flow regulation by laser Doppler flowmetry, iontophoresis and curve analysis, contribution of axon reflex," *Microvasc. Res.* **67**, 207–214 (2004).
10. R. T. de Jongh, E. H. Serne, R. G. IJzerman, G. de Vries, and C. D. Stehouwer, "Impaired microvascular function in obesity, implications for obesity-associated microangiopathy, hypertension and insulin resistance," *Circulation* **109**, 2529–2535 (2004).